Simultaneous Skeletonization and Topologic Decomposition for Digital Shape Reconstruction

Tilman Wekel and Olaf Hellwich
TU-Berlin
Marchstrasse 23
Germany, 10587 Berlin
{olaf.hellwich|t.wekel}@tu-berlin.de

ABSTRACT

Analyzing the structure of 2D shapes has been studied intensively in recent years. It is a key aspect in various computer vision and computer graphics applications. In this paper, a new algorithm is proposed which efficiently computes a skeleton and a corresponding decomposition of an arbitrary shape. Given the Voronoi diagram, the pruning step has linear complexity. The skeleton is a sparse 1D representation which captures the topology as well as the general structure of a shape. Considering the Voronoi diagram of the boundary vertices, the skeleton is extracted as a subset of the Voronoi edges using a simple classification scheme. A parameter allows to control the skeleton's sensitivity to perturbations in the boundary curve. The dual Delaunay triangulation yields a topological decomposition of the shape that is consistent with the skeleton. Each part can be classified as belonging to one of three base types which have some interesting properties. The method has been successfully implemented and evaluated. The presented concepts can also be applied to manifold surfaces which is particularly useful for digital shape reconstruction as it is shown at the end of this paper.

Keywords

skeletonization, shape decomposition, topology, Voronoi diagram

1 INTRODUCTION

A skeleton is a 1D representation of a shape that can be intuitively compared to a stick figure. The skeleton captures the topological structure of a shape. It is used as a compact descriptor for various applications such as shape classification or geometric modeling. According to Andrés et al., related approaches can be associated to one of three categories: driven by shape thinning, distance transform-based and methods that use the Voronoi diagram of the boundary points [SM12]. Thinning algorithms iteratively shrink the shape until it is degenerated to a line. The method is commonly applied in digital image analyses, where the discrete nature of the data allows a precise definition of connectivity and thinness. Recently, the idea has been transferred to 3D voxel data [HL10]. Thinning algorithms often have a lack in performance or produce disconnected skeletons. They typically work on discrete pixel-based data and it would be difficult to adapt them to continuous domains. Aicholzer et al. introduce the straight skeleton which is constructed by contracting the boundary towards the interior of the shape [Aic96][CV12]. Distance transform-based algorithms compute a distance map for the interior region of the shape. The map associates a scalar value to each point, where the scalar value is the distance to the closest boundary point [RS04]. These methods allow a geometrically accurate construction of the medial axis. In a pruning step, unwanted branches are deleted while the topology of the remaining skeleton needs to be preserved [XB07]. Amenta et al. uses the medial axis to reconstruct a surface from a 3D point-cloud [NA01]. Voronoi-based methods evolve the fact, that the Voronoi diagram of the boundary points consists of edges that are bisectors of opposing boundary points. In the approach of Ogniewicz et al., the relevance of each edge is computed based on the maximally filling disk and the chord length of the corresponding boundary segment. Compared to our approach, the algorithm invokes computationally expensive processing steps such as the estimation of the maximally filling disk. In a similar approach, Brandt and Algazi introduce a method to estimate the minimum sampling density for the boundary points [Bra92]. Beeson et al. use the minimum spanning tree for the pruning step [PB05]. Algorithms for shape decomposition are often inspired by psychology and human perception [JL06b]. The work proposed by Lien et al. efficiently decomposes arbitrary shapes in approximately convex shapes [JL06a]. Rosin proposes a partitioning scheme based on a simple convexity measure which is calculated as the ratio of the area of the shape itself and the area of its convex hull [Ros00]. The decomposition scheme presented by Liu et al. is based on convexity and Morse theory [HL10]. Lien et al. presents an approach, where a skeleton and a decomposition are computed alternatively [JL06b]. Our approach yields some significant advantages. Given an arbitrary shape and its Voronoi-diagram, the pruning is computed in linear time with respect to the number of boundary points. The presented scheme elegantly connects skeleton and decomposition based on the duality between Voronoi diagram and Delaunay triangulation. Based on the work of Aigner et al., the shape is decomposed into a set of topologically meaningful parts which is useful for digital shape reconstruction, registration or classification [WA12]. Compared to Aigner et al., skeletonization and decomposition is computed simultaneously and the estimation of a maximally filling disk is not required.

2 SKELETON EXTRACTION

As stated, the skeleton is a suitable 1D-representation of a shape. Clearly, there is a relation to the Voronoi diagram, where each Voronoi edge is an equidistant bisector of two points. In the following it is shown, how the skeleton can be constructed based on the Voronoi diagram of the boundary points. Consider an arbitrary shape $\mathbf{S} \in \mathbb{R}^2$, which is given by a set of closed, continuous and non-intersecting boundary curves $\partial\mathbf{S} = \{C_0, \ldots, C_n\}$. For the sake of simplicity, a curve is assumed to be given in a parametrized form: $C_i(t_i), t_i \in [0 \ldots 1]$. Each curve of $\partial\mathbf{S}$ is approximated by a set of points $\mathbf{V} = \{V_0, \ldots, V_n\}$. All points in $V_a \in \mathbf{V}$ lie on the respective curve: $\{\forall v_i \in V_a : v_i = C_a(t_i)\}$, where t_i is the associated parameter. A given point $v \in \mathbb{R}^2$ is either classified as lying inside or outside the shape, $\mathscr{L}(v) \in \{l_I, l_O\}$. Consider an open curve segment which is defined to be the shortest curve between two vertices lying on the same curve: $C_a[t_i, t_q], \{v_i, v_q\} \in V_a$. The situation is visualized in (a) of Figure 1. The arc length of this curve segment can be computed by: $L(C_a[t_i,t_q]) = \int_{t_i}^{t_q} \|\dot{C}(t)\| dt$. According to Ogniewicz et al., curve potentials are an elegant way to calculate the arc length of an arbitrary curve segment [RO95]. Given a curve C_a, an arbitrary reference point v_0 is defined. The curve potential of a point v_i with the corresponding parameter t_i is given by: $\phi_a(v_i) = L(C_a[v_0, v_i])$. $\phi_a(v_i)$ needs to be calculated only once for each boundary point. A weight

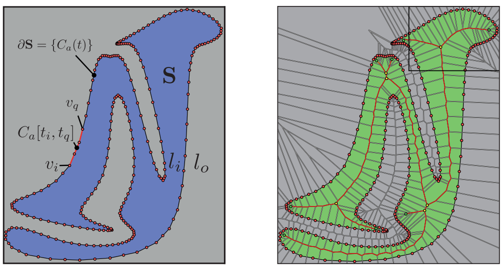

(a) (b)

Figure 1: Shape boundary (a) and Voronoi diagram (b).

function $\omega(\cdot,\cdot)$ that corresponds to the arc length of a curve segment is introduced as:

$$\omega(v_i, v_q) = \begin{cases} \|\phi_a(v_i) - \phi_a(v_q)\| & \text{if } v_i, v_q \in V_a \\ \infty & \text{otherwise.} \end{cases} \quad (1)$$

It can be efficiently calculated based on a difference of potentials. Note that the function $\omega(\cdot,\cdot)$ is defined to be infinity if the vertices do not belong to the same curve. The boundary vertices V define the sites of a Voronoi diagram D. The Voronoi diagram consists of vertices, edges, sites and regions: $D = \{\tilde{V}, \tilde{E}, \tilde{S}, \tilde{R}\}$. All elements of the Voronoi diagram are indicated by a tilde. The sites are given by the boundary vertices. Let $\tilde{s}_i = v_i$ and $\tilde{s}_j = v_j$ be two sites, then all points which are closer to $\tilde{s}_i$ than to $\tilde{s}_j$ can be defined as: $\tilde{r}_{ij} = \{p \in \mathbb{R}^2 : \delta(p, \tilde{s}_i) < \delta(p, \tilde{s}_j)\}$. Where $\delta(.,.)$ is the distance function. The corresponding Voronoi region $\tilde{r}_i$ is then the set of all points which are closer to $\tilde{s}_i$ than to any other site: $\tilde{r}_i = \bigcap_{i \neq j} \tilde{r}_{ij}$. The Voronoi regions meet at Voronoi edges which can be seen as equidistant bisectors of their adjacent sites. A plot of the problem can be seen in (b) of Figure 1. The skeleton $\tilde{F}$ is defined as a subset of the Voronoi diagram. $\tilde{F}$ is a graph structure that consists of vertices and edges, $\tilde{F} = \{\tilde{V}, \tilde{E}\}$. A Voronoi edge $\tilde{e}_o$ is associated with its corresponding source and target vertex $\{\tilde{v}^s(\tilde{e}_o), \tilde{v}^t(\tilde{e}_o)\}$ and its right and left site $\{\tilde{s}^r(\tilde{e}_o), \tilde{s}^l(\tilde{e}_o)\}$. $\tilde{e}_o$ is classified as belonging to the skeleton $\tilde{e}_o \in \tilde{F}$, if the following conditions are fulfilled:

1. The Voronoi edge must have a source and a target vertex: $(\tilde{v}^s(\tilde{e}_o) \neq \emptyset) \cap (\tilde{v}^t(\tilde{e}_o) \neq \emptyset)$.
2. The source and the target vertex must lie inside the shape: $(\mathscr{L}(\tilde{v}^s(\tilde{e}_o)) = l_I) \cap (\mathscr{L}(\tilde{v}^t(\tilde{e}_o)) = l_I)$.
3. Consider the boundary points that correspond to the sites: $\tilde{s}^r(\tilde{e}_o) = v_r, \tilde{s}^l(\tilde{e}_o) = v_l$. The weight of the points has to be larger than a defined threshold: $\omega(v_r, v_l) > \omega_{min}$.

The edge classification scheme is visualized in (a) of Figure 2. The first and second condition imply that the resulting skeleton lies inside the corresponding shape. The classification can be performed for each edge which implies linear complexity $\mathscr{O}(n)$ with respect to the number of Voronoi edges. The computation of the Voronoi diagram has a complexity of $\mathscr{O}(n \log n)$.

3 SEGMENT GRAPH

Given a skeleton $\tilde{F} = \{\tilde{V}, \tilde{E}\}$, each vertex is associated with a degree $d(\tilde{v})$ that gives the number of adjacent skeleton edges. According to the properties of the Voronoi diagram, the degree of a vertex $\tilde{v} \in \tilde{F}$ is either one, two or three, $d(\tilde{v}) \in \{1,2,3\}$. Edges which are adjacent to at least one vertex with a degree not equal to two are defined as bridges: $\tilde{E}_b$: $\{\forall \tilde{e}_o \in \tilde{E}_b : d(\tilde{v}^s(\tilde{e}_o)) \neq 2 \cup d(\tilde{v}^t(\tilde{e}_o)) \neq 2\}$. $\tilde{E}_b$ implies a decomposition of the skeleton, such that each part only contains vertices of the same degree. A is introduced as the Delaunay triangulation which is dual to the underlying Voronoi diagram of the boundary points: $D \leftrightarrows A$. All elements of the Delaunay triangulation are indicated by a hat. A bridge $\tilde{e}_b \in \tilde{F}$ is now associated with its dual Delaunay edge: $\tilde{e}_b \leftrightarrows \hat{e}_b$. $\hat{e}_b$ is referred as separator edge. $\hat{e}_b$ connects two boundary vertices and splits the shape into two parts. The set of all bridges and their corresponding separator edges decomposes the skeleton and the shape into a set of three different types of parts: $\mathbf{S} = \{{P_0}^{j,t,l}, \ldots, {P_m}^{j,t,l}\}$:

1. *Junction*. A junction P^j is given by a single vertex $\tilde{v}_j, d(\tilde{v}_j) = 3$ and its dual Delaunay triangle: $\tilde{v}_j \leftrightarrows \hat{t}_j$. $\hat{t}_j$ coincides with the three adjacent separator edges.

2. *Terminal*. A vertex with the degree of one $\tilde{v}_t, d(\tilde{v}_t) = 1$ yields a terminal part P^t. Consider the dual Delaunay triangle: $\tilde{v}_t \leftrightarrows \hat{t}_t$. The boundary of P^t is now given by the adjacent separator edge $\hat{e}_t$ and the curve segment of the corresponding boundary curve that passes through the vertices of $\hat{t}_t$.

3. *Linear*. A linear part P^l represents a branch that is defined by a linear sequence of edges, $\tilde{E}_l$: $\{\forall \tilde{e}_o \in \tilde{E}_l : d(\tilde{v}^s(\tilde{e}_o)) = d(\tilde{v}^t(\tilde{e}_o)) = 2\}$. The adjacent separator edges define a left and a right segment on the corresponding boundary curves.

Now, G is introduced as the segment graph, where the set of all parts represents the nodes of G. The edges of G are given by the bridges and their respective separator edges. The resulting decomposition into junctions (yellow), terminal (green) and linear parts (purple) as well as the corresponding segment graph is visualized in (b) of Figure 2. The dashed lines represent the bridges (black) and the separator edges (white).

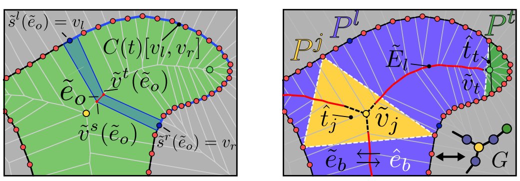

(a) (b)

Figure 2: Topology of a Voronoi edge (a) and semantic decomposition (b).

4 EVALUATION AND APPLICATION

In this section, the presented algorithm is applied to various shapes which are taken from the MPEG-7 library [TZ01]. The decomposition as well as the skeleton is compared with competitive algorithms [JL06a][PB05]. The results are shown in Figure 3. The skeleton computed based on the approach of Beeson et al. can be found in (a), the convex shape decomposition corresponds to (b) and the combined outcome of our method is to be found in (c). The skeleton in (c) clearly reflects the most important features of the boundary curve while unimportant details are ignored. Each junction in the skeleton yields a triangle (yellow) which allows to decompose the shape into compact and meaningful parts along its topology. The approach based on approximate convexity has several disadvantages. The overall structure of the decomposition is very sensitive to small perturbations in the boundary curve as it can be seen in (1,b). While the shape of each spike of the star is almost similar, the decomposition varies significantly. Moreover, the decomposition is often characterized by a bad scaling (3,b). Some small regions such as the neck or the upper part of the hind legs are heavily oversegmented. The approach presented by Beeson et al. is designed for grid-based data structures only. The resulting skeleton appears to be quite sensitive to small deformations of the shape as it can be seen in (1,a). The inner part of the skeleton looks not very symmetrical while the shape itself has a symmetric structure. The skeleton in (c) looks much smoother especially at vertices where multiple branches intersect. The presented approach has been developed in the context of digital shape reconstruction, where CAD (Computer aided design) models are reconstructed from triangulated surfaces. Man-made objects can be seen as a composition of smooth surface patches which meet at curved

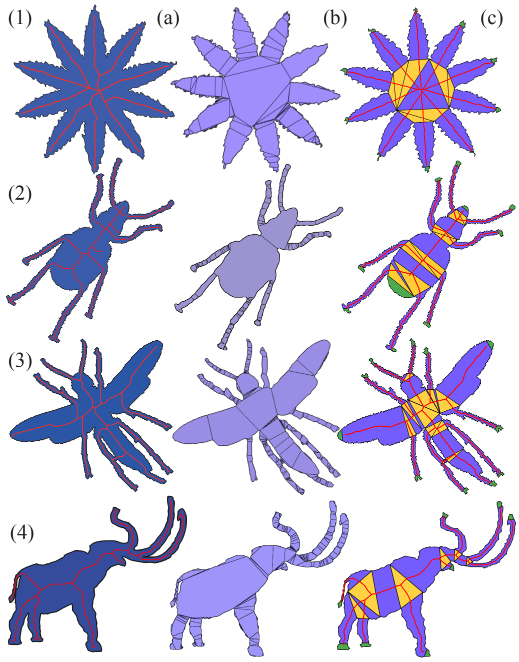

Figure 3: Comparison of the presented method (c) with the approach of Beeson et al. (a) and Lien et al. (b).

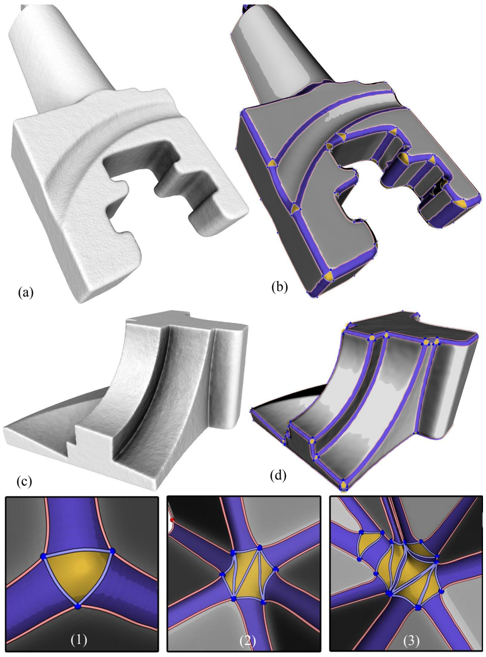

Figure 4: The decomposition is applied in digital shape reconstruction.

regions. The approach presented by Wekel et al. is used to segment and classify the surface into smooth and critical regions [TW13]. These regions represent a skeleton that captures the topology of a triangulated surface. In order to describe the model by typical CAD entities such as vertices, curves and parametric surfaces, it is important to decompose the polyhedral surface into a set of reasonable components. The reconstructed CAD models can be seen in (b) and (d) of Figure 4. Smooth surface patches are described by trimmed b-spline surfaces (grey). Using the presented algorithm, the blending regions are decomposed into junctions (yellow) and linear segments (purple). The presented method can be directly transferred to the domain of 2D manifolds in $\mathbb{R}^3$. As described in Section 3, each resulting part is characterized by a unique and compact structure which enables a straight forward representation in common CAD systems. The images (1), (2) and (3) in Figure 4 demonstrate, how the Voronoi-based approach allows to uniquely decompose even complex junctions into a set of simple, triangular surfaces and linear parts.

5 REFERENCES

[Aic96] Aurenhammer F. Alberts D. Gärtner B. Aichholzer, O. A novel type of skeleton for polygons. In A. Salomaa H. Maurer, C. Calude, editor, *J.UCS The Journal of Universal Computer Science*, pages 752–761. Springer Berlin Heidelberg, 1996.

[Bra92] Algazi R. Brandt, J. Continuous skeleton computation by voronoi diagram. *CVGIP: Image Understanding*, 55(3):329 – 338, 1992.

[CV12] B. Weber J. Halatsch D. Aliaga C. Vanegas, T. Kelly. Procedural generation of parcels in urban modeling. *Comp. Graph. Forum*, 31(2pt3):681–690, May 2012.

[HL10] L. Latecki H. Liu, W. Liu. Convex shape decomposition. In *CVPR, 2010 IEEE Conference on*, pages 97 –104, june 2010.

[JL06a] N. Amato J. Lien. Approximate convex decomposition of polygons. *Comput. Geom. Theory Appl.*, 35(1):100–123, August 2006.

[JL06b] N. Amato J. Lien, J. Keyser. Simultaneous shape decomposition and skeletonization. In *Proc. of the 2006 ACM symposium on Solid and physical modeling*, SPM '06, pages 219–228, New York, NY, USA, 2006. ACM.

[NA01] S. Choi R. Kolluri N. Amenta, Nina. The power crust. In *Proc. of the sixth ACM symposium on Solid modeling and applications*, SMA '01, pages 249–266, New York, NY, USA, 2001. ACM.

[PB05] B. Kuipers P. Beeson, N. Jong. Towards autonomous topological place detection using the extended voronoi graph. In *IEEE ICRA05*, pages 4373–4379, 2005.

[RO95] O. Kübler R. Ogniewicz. Hierarchic voronoi skeletons. *Pattern Recognition*, 28(3):343 – 359, 1995.

[Ros00] P. Rosin. Shape partitioning by convexity. *Systems, Man and Cybernetics, Part A: Systems and Humans, IEEE Transactions on*, 30(2):202 –210, mar 2000.

[RS04] A. Telea R. Strzodka. Generalized distance transforms and skeletons in graphics hardware. In *VisSym*, pages 221–230, 2004.

[SM12] J. Lang S. Montero. Smi 2012: Full skeleton pruning by contour approximation and the integer medial axis transform. *Comput. Graph.*, 36(5):477–487, August 2012.

[TW13] O. Hellwich T. Wekel. Voronoi-based extraction of a feature skeleton from noisy triangulated surfaces. In *ACCV2012*, volume 7725 of *Lecture Notes in Computer Science*, pages 108–119. Springer Berlin Heidelberg, 2013.

[TZ01] F. Preteux T. Zaharia. 3d-shape-based retrieval within the mpeg-7 framework. pages 133–145, 2001.

[WA12] B. Jüttler W. Aigner, F. Aurenhammer. On triangulation axes of polygons. *European Workshop on Computational Geometry*, 28:125–128, 2012.

[XB07] W. Liu X. Bai, J. Latecki. Skeleton pruning by contour partitioning with discrete curve evolution. *IEEE PAMI*, 29:449–462, 2007.